Received: 24 April 2025 | Accepted: 18 November 2025

DOI: 10.1111/1365-2664.70251

Journal of Applied Ecology

RESEARCH ARTICLE

Successional and native forests predict the occurrence and infection status of Chagas disease vectors in Panama

Juliana Hoyos[1,2] | Azael Saldaña[3] | Sonia Altizer[1,2] | Vanessa Pineda[4] | Kadir Gonzalez[4,5] | Jose E. Calzada[4] | Raissa Nogueira de Brito[6] | Susan Tanner[6] | Daniel Mendieta[4] | Alberto Cumbrera[4] | Nicole L. Gottdenker[2,7]

[1]Odum School of Ecology, University of Georgia, Athens, Georgia, USA; [2]Center for the Ecology of Infectious Diseases, University of Georgia, Athens, Georgia, USA; [3]Centro de Investigación y Diagnóstico de Enfermedades Parasitarias (CIDEP), Facultad de Medicina, Universidad de Panamá, Panama City, Panama; [4]Departamento de Investigación en Parasitología, Instituto Conmemorativo Gorgas de Estudios de la Salud, Panama City, Panama; [5]Departamento de Microbiología, Facultad de Medicina, Universidad de Panamá, Panama City, Panama; [6]Department of Anthropology, University of Georgia, Athens, Georgia, USA and [7]Department of Pathology, University of Georgia College of Veterinary Medicine, Athens, Georgia, USA

Correspondence
Juliana Hoyos
Email: julianah.2108@gmail.com

Funding information
Ministerio de Ciencia, Tecnología e Innovacion de Colombia (MinCiencias), Grant/Award Number: Convocatoria Doctorados en el Exterior 906; National Science Foundation, Grant/Award Number: CNH2-1924200

Handling Editor: Bret Elderd

Abstract

1. Changes in land use and land cover (LULC) due to agricultural expansion, commercial land management and other human-driven modifications significantly influence the ecology of pathogens and vectors. This underscores the urgent need to understand how these respond to rapid and dynamic land use changes in these ecosystems and, critically, to identify strategies for mitigating their impacts.
2. In tropical Central and South America, palm trees serve as primary habitats for *Rhodnius* kissing bugs, vectors of *Trypanosoma cruzi*, the etiologic agent of Chagas disease. This study investigates how LULC, weather and traits of the palm *Attalea butyracea* predict the occurrence and infection of *Rhodnius pallescens*, integrating field data collection, molecular detection and spatial and hierarchical analyses across a rural landscape in Panama.
3. *Rhodnius pallescens* were collected from 46 palms in 11 communities with different landscape compositions including native forests, grasslands, successional forests and artificial structures. Robust occupancy modelling using land cover data at 10 m^2 resolution revealed that successional forest cover at 300 m spatial scale predicted greater occurrence of *R. pallescens*, whereas native forest predicted lower occurrence. Quadratic models outperformed linear models, indicating occupancy peaks at intermediate land covers and palm tree traits.
4. Real-time PCR assays detected *Trypanosoma* infections in 70% of *R. pallescens* across communities. Spatial autocorrelation analyses showed significant spatial clustering for *T. cruzi* but not for *Trypanosoma rangeli*. We used generalized additive mixed models to assess the influence of palm-level and landscape-scale attributes on parasite infection and identified significant nonlinear positive

This is an open access article under the terms of the Creative Commons Attribution License, which permits use, distribution and reproduction in any medium, provided the original work is properly cited.
© 2025 The Author(s). *Journal of Applied Ecology* published by John Wiley & Sons Ltd on behalf of British Ecological Society.

associations between *T. cruzi* infection and native forest and grassland, with high predictive accuracy (AUC = 0.90).

5. *Synthesis and applications*. Findings here show that successional forest predicts greater kissing bug infestation risk in palm trees, whereas native forest predicts lower kissing bug occurrence but greater infection with *T. cruzi*. These insights can guide land use planning towards vegetation management practices that help minimize *T. cruzi* transmission risks for rural communities. Importantly, vector surveillance should target forest-grassland ecotones and consider forest successional stages near settlements, with intensified monitoring after disturbances; this approach is applicable to other vector-borne pathogen systems shaped by land use change.

KEYWORDS
Chagas disease, cover, deforestation, kissing bug, land reversion, land use change, *Rhodnius pallescens*, *Trypanosoma cruzi*

1 | INTRODUCTION

Chagas disease, caused by the vector-borne parasite *Trypanosoma cruzi*, is one of the most prevalent communicable tropical diseases in Latin America, and a significant cause of morbidity and mortality in humans (Pan American Health Organization [PAHO], 2023). The *T. cruzi* parasites are mainly transmitted via the infected faeces of blood-sucking triatomine kissing bugs. This transmission mode remains the main route in endemic regions across continental Latin America (Cucunubá et al., 2024). In tropical countries, palm trees are a key ecological niche for triatomine (kissing bug) vectors of Chagas disease in the genus *Rhodnius* (Abad-Franch et al., 2015; Carcavallo et al., 1998). Landscape disturbances impact the presence of palms and the abundance of palm-dwelling bugs, both of which are indicators of Chagas disease transmission risk in rural areas (Gottdenker et al., 2011; Lent & Wygodzinsky, 1979; Santos et al., 2021). In many tropical and subtropical landscapes of the Americas, certain palms, such as *Attalea* spp., are often found near human settlements associated with past and present anthropogenic disturbances (Calderón & González, 2020; Mertzlufft et al., 2020; Wright et al., 2000). Palm infestation by *Rhodnius* species is common, and peridomestic palms are key sources of wild triatomines invading human dwellings (Santos et al., 2021). Palm tree crowns have an intricate structure that establishes a microenvironment favourable for triatomines (Varian et al., 2023; Urbano et al., 2015; Teixeira et al., 2001; Abad-Franch et al., 2015). This palm crown complexity fosters a stable microclimate and provides shelter and surfaces suitable for insect breeding (Dias et al., 2011).

Habitats with palm trees also favour the presence of wild mammal hosts, which are blood sources for triatomines (Gottdenker et al., 2011) and influence the prevalence of *T. cruzi* infection; among these mammals, marsupials are particularly important, as they are key reservoirs for the parasite and play a crucial role in maintaining the sylvatic enzootic cycle (Teixeira et al., 2001). Along with *T. cruzi*, a closely related species, *Trypanosoma rangeli*, overlaps geographically and shares many of the same triatomine vectors and vertebrate hosts (Botero et al., 2010). *Trypanosoma rangeli* is considered non-pathogenic to humans but can cause pathogenic effects in triatomine bugs, affecting their survival and reproduction (Guhl & Vallejo, 2003). Co-infections with *T. cruzi* and *T. rangeli* are common in vector populations and have complex effects on both parasite transmission and vector fitness (Peterson et al., 2016). Additionally, both parasites indicate contrasting habitat responses linked to landscape disturbance and host community composition (Gottdenker et al., 2016).

Anthropogenic impacts like land use and climate change can alter the transmission of Chagas disease, as other vector-borne diseases (Burkett-Cadena & Vittor, 2018; Gottdenker et al., 2014; Keesing et al., 2010; MacDonald & Mordecai, 2019; Vaz et al., 2007). The effects of this land conversion depend on the type and rate of change, as well as traits of the vector, host and parasite (Ferraguti et al., 2023). In Panama, Gottdenker et al. (2012) found that infection rates in Triatominae were higher in disturbed landscapes than in protected forests due to shifts in host life histories. Life history theory suggests long-lived mammals in intact forests invest more in immunity, while disturbed areas favour fast-reproducing species that increase pathogen transmission (Tonelli et al., 2024). However, Dumonteil and Gourbiére (2004) found the highest infection in kissing bugs occurred in mature forests in the Yucatan Peninsula, aligning with the zoonotic origin of *T. cruzi*.

In Neotropical regions, successional forests cover about one-third of the land and continue to expand (Chazdon et al., 2016). These regenerating forests support high biodiversity but represent only part of the regional species pool (Rozendaal et al., 2019). While reforestation offers social and ecological benefits, it may also increase disease spread when native forests are replaced by monocultures like oil palm (Morand & Lajaunie, 2021). Forest regeneration can influence pathogen dynamics depending on species resilience

and restoration speed (Vinson et al., 2022; Prist et al., 2023). Rapid vertebrate community recovery may reduce zoonotic transmission (Keesing & Ostfeld, 2021), whereas slow regeneration could maintain human-adapted vectors (Eisen et al., 2017). Additionally, regeneration may create new vector habitats and increase human exposure (Athni et al., 2021; Poorter et al., 2024; Roche et al., 2013). A key research gap concerns how forest transitions affect vector-borne diseases like Chagas (Skaff et al., 2017), especially given nonlinear infection patterns across disturbance gradients (Vinatier et al., 2013).

Here, we used a combination of field collected data and molecular diagnostics to study Chagas disease vectors inhabiting rural areas to understand how landscape composition and forest regeneration influence vector occurrence, infection and risk of pathogen transmission. By quantifying both fine-scale landscape and microhabitat components and larger-scale weather conditions, we tested associations between climate, deforestation and land reversion, vector habitat preferences, and infection patterns of two species of *Trypanosoma* in the triatomine vector *Rhodnius pallescens* in palm trees in rural Panama. Based on previous studies, summarized in Table S1, we predicted that both vector and parasite will respond to environmental covariates, including successional forest, native forest and pasture. Using our field observations and molecular parasite detection, we developed robust hierarchical models that considered the potential for linear and nonlinear relationships as well as the risks of imperfect detection and spatial autocorrelation. With our approach, we highlight the importance of recognizing the landscape as a dynamic and intricate mosaic composed of various land cover types. Building on our findings, we provide key information on how dynamic habitat changes-specifically, reforestation and deforestation-affect the occurrence and likelihood of infection of Chagas disease vectors. This information could help guide targeted control and mitigation measures to lessen the spread of the disease in rural areas.

2 | METHODS

2.1 | Ethical approval

Kissing bug collections were conducted in compliance with institutional and national ethical guidelines. Approval was granted by the University of Georgia Institutional Animal Care and Use Committee (IACUC; Protocols A2023 07-015-Y2-A0 and A2022 07-008-Y3-A0). Additional authorization was obtained from the Instituto Conmemorativo Gorgas de Estudios de la Salud IACUC (Nota 001/CIUCAL/ICGES22) and the Panamanian Ministry of Environment (MiAMBIENTE) under permit ARBG-009-2022.

2.2 | Study sites

For this study, we selected 11 communities within the province of Cocle in Panama (Figure 1), an area characterized by many ecosystems, dominated by moist forests in the lowlands, especially along the Pacific slope, key hydric resources and protected areas belonging to the Sistema Nacional de Áreas Protegidas (Panamá's National Protected Areas System). This province has been greatly affected by human activities: Data from Global Forest Watch (GFW, 2024) indicates that between 2002 and 2023, Coclé lost 2.10 kha of primary rainforest, which represents 6.1% of the total loss of its tree cover in the same period, and the total area of primary rainforest in Coclé decreased by 5.5%. From 2000 to 2020, the largest change in tree cover corresponded to (a) decline in stable forest (forests that are at least 1 km from the forest edge) (215 kha), (b) increase in disturbed forest (27.6 kha), (c) total forest area loss (17.7 kha) and (d) forest gain in some locations (4.07 kha). Within this area, we sampled locations that covered different habitat types, land use and land cover (LULC) compositions, and topographic features while controlling for similar socio-economic structure. Details on how LULC compositions were characterized across sampling locations are described in a later section. Sites were spaced to ensure adequate coverage of the study area and to account for logistical constraints (e.g. accessibility for sampling palm crowns with a ladder).

2.3 | Kissing bug collections

For Triatomine sampling, 46 *Attalea* palms were opportunistically selected across the 11 communities (1–10 palms per community; Figure 1). Vectors were captured using 3 mouse-baited traps (Noireau et al., 2002) per palm, totalling 138 traps per visit. We sampled palms twice during the dry season (March 2022 and 2023) and twice during the rainy season (November 2022 and December 2023). Traps were placed inside each palm crown on opposing sides for a single night during each visit from 18:00 to 6:00. Triatomines were placed in 100-mL plastic containers and later transferred to tubes with molecular grade ethanol, recording the developmental stage and the species of triatomine (Lent & Wygodzinsky, 1979).

2.4 | Environmental covariates

Macroclimatic data (precipitation and temperature) were obtained for each sampling area at each sampling period using the Giovanni system at the NASA Goddard Earth Science Center Data and Information Services Center. Daily mean precipitation rates were analysed using the Precipitation Measurement GPM Level 3 IMERG daily data at 10 × 10 km (GPM_3IMERGDF) derived from the half-hour GPM_3IMERGHH. We obtained daily average, minimum and maximum temperature data from the MERRA-2 M2SDNXSLV dataset (Global Modeling and Assimilation Office (GMAO), 2015).

LULC types were coded as a continuous variable, reflecting the reality of fragmented landscapes and to avoid misclassification bias. We used high spatial resolution data published in the MiAMBIENTE Panama Forest Cover and Land Use 2021 database (including 10 m resolution Sentinel-2 data) and reclassified it into

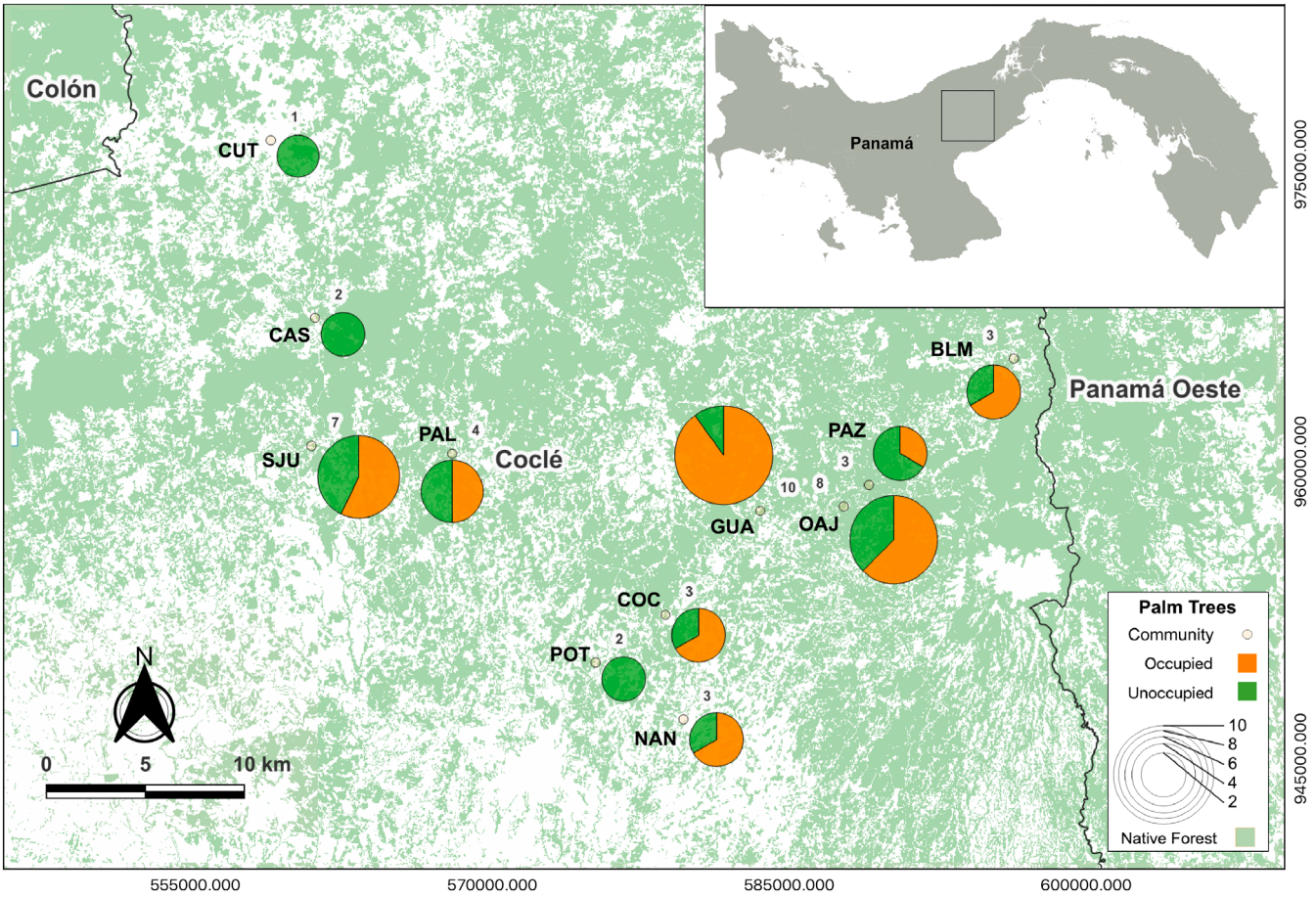


FIGURE 1 Locations of the 11 study communities in Coclé Province, Panama. Pie charts show the proportion of *Attalea* palms occupied by *Rhodnius pallescens* (orange) in each community, with the accompanying numbers and pie sizes indicating the number of palms sampled per site. Light-green pixels represent native forest cover across the study landscape.

five categories proposed by the United Nations Convention to Combat Desertification from the SDG 15.3.1 reports (Supporting Information S1). For each *Attalea* palm sampled, we extracted land cover and land use values within three different buffer sizes (100, 300 and 500 m in radius) based on the flight capacity of *R. pallescens* (Castro et al., 2014). We then estimated the percentage of each land cover class by dividing the number of pixels for each land cover class by the total number of pixels per area as illustrated in Figure 2. All spatial analyses were conducted on the Google Earth Engine platform. Correlations between LULC covariates were evaluated through Pearson coefficients using a cut-off value of $r \geq 0.70$, discarding the variable that was less correlated with the dependent variable for downstream ecological modelling (Figures S1–S3). We retained all land cover covariates due to nonsignificant observed correlation.

We recorded individual-palm traits and microhabitat characteristics including the following: (1) elevation, (2) stem height, (3) the semi-quantitative 'dead organic matter score' (DOM score hereafter), a measure used to quantify the amount of decomposed organic matter present in the palm tree crown and used as an indicator of moisture stability in the microhabitat based on descriptions by Abad-Franch et al. (2005) ranging on a scale from 1 (little or no matter) to 4 (abundant matter), (4) the amount of infructescence as described by Varian et al. (2023) and Abad-Franch et al. (2015) and (5) the number of connected tree palms, that is the number of palms located within a radius of 50 m around the sampled palm. Palm traits were standardized to a mean of zero and standard deviation (SD) of one for downstream ecological modelling. We modelled the influence of these variables on the occupancy probabilities of kissing bugs (see below) considering a hypothesis-driven approach. The summary of these assumptions is depicted in Table S1. To minimize overlap, palm trees were spaced at least 400 m apart, resulting in only minimal overlap among 300-m buffers, and we confirmed that such overlap did not bias results through spatial autocorrelation analyses (described later). Additionally, we explored potential correlations between individual-palm traits and LULC types (Figure S4).

2.5 | Molecular testing for parasite detection

We performed molecular diagnostics with high sensitivity and specificity on Triatomine samples to distinguish between *T. cruzi* and *T. rangeli*. Collected *Rhodnius* whole bodies were crushed for genomic DNA extraction using phenol–chloroform–isoamyl alcohol. Genomic

BRITISH ECOLOGICAL SOCIETY Journal of Applied Ecology

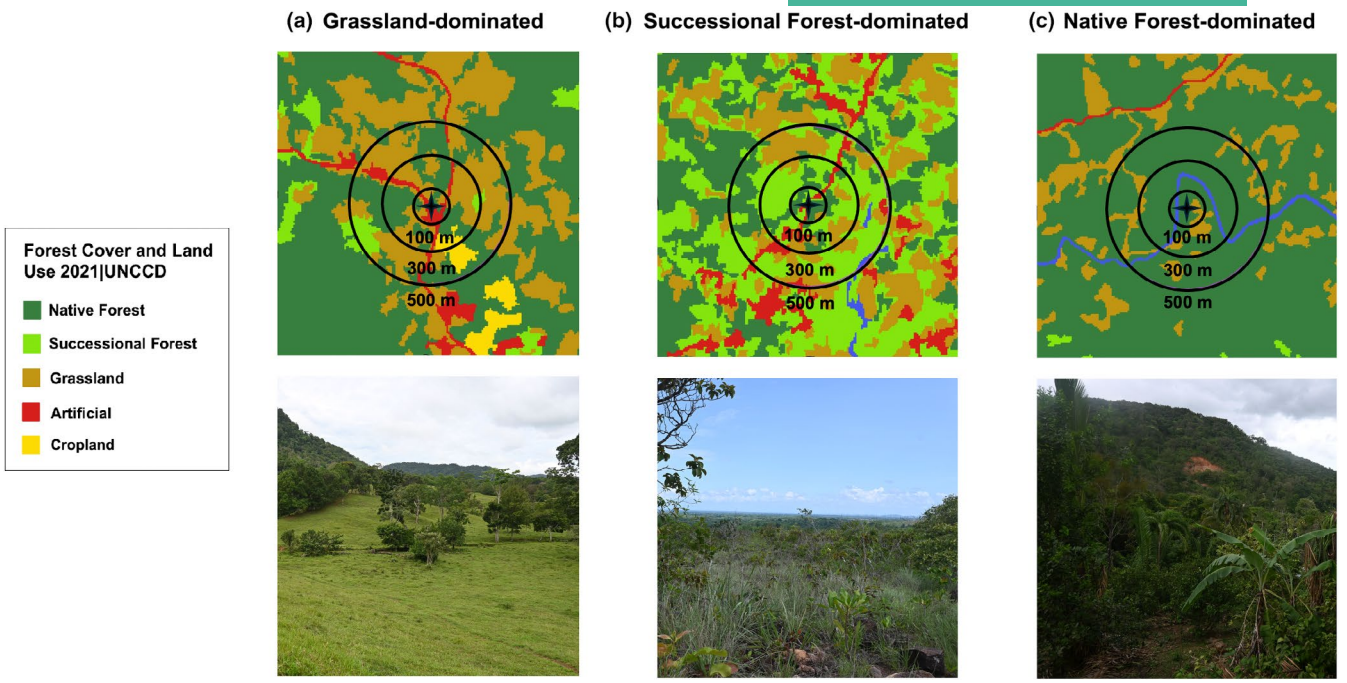


FIGURE 2 Variation in landscape configuration among study sites. Land cover categories proposed by the United Nations Convention to Combat Desertification were calculated within the 100-, 300- and 500-m radii from the centroid (each one of the *Attalea* palms sampled). The figure represents: (a) areas with dominance of grassland (b) areas with dominance of successional forest and (c) areas with dominance of native forest. Photographs are from actual sampling locations that correspond to each study site.

DNA was analysed for the simultaneous presence of *T. cruzi* and *T. rangeli* rDNA by amplifying segments of the 24Sα subunit of both species in a real-time PCR assay generating 140 and 175 bp fragments using conditions adjusted from Muñoz-Calderón et al. (2020). Each reaction consisted of 3 μL of extracted DNA, primers D75b and D76b each at a final concentration of 0.9 μM, probes TrTq and TcTq at concentrations of 0.125 and 0.095, respectively, and FastStart Universal Probe Master Mix (Roche Diagnostics, Mannheim, Germany) in a final volume of 20 μL using a Bio-Rad CFX96 instrument whose cycling conditions were an initial 10 min step at 95°C and 40 cycles at 95°C for 30 s and 60°C for 1 min. The quality of the machine-calculated thresholds and reaction curves was visually checked. Samples with Cq values below 37 were considered positive.

2.6 | *Rhodnius pallescens* site-occupancy analysis

We determined the proportion of locations where kissing bugs were detected at least once across the four sampling visits (MacKenzie et al., 2006) and modelled *R. pallescens* occupancy probability as a function of the above LULC proportions, palm traits and different spatial extends using single-species occupancy models in the R package spOccupancy (Doser et al., 2022). An occupancy model consists of two sub-models: (Abad-Franch et al., 2005) an observation model that specifies the observed detection-no detection data, conditional on the true presence–absence of the species, detection probability (p) (MacKenzie et al., 2002); and (Abad-Franch et al., 2010) an ecological process model that describes the true, partially observed presence or absence of a species as a function of covariates, occupancy probability (ψ). Here, we used a first set of detection covariates corresponding to climate variables during the sampling time, and a second set of occurrence covariates, consisting of landscape composition analysis and palm traits described above. To account for potential spatial autocorrelation among our survey locations, and the associated bias in parameter estimates, we compared Bayesian spatial and non-spatial versions of our top candidate models. A complete description of the model parameters is described in Supporting Information S1.

We developed models with additive combinations of covariates (Table S2), along with a null model for occupancy sub-models using only average daily temperature during the sampling period as a covariate in the detection sub-model. We calculated the posterior mean and SD of the model coefficients with 90% Bayesian credible intervals (BCI). Parameter estimates of covariates with BCI that did not cross 0 were considered important predictors of species occupancy, as this was reflective of a consistent relationship within model iterations. We computed Bayesian p-values with the Freeman–Tukey statistic to assess model fit, where a model with a good fit to the data had a value near 0.5, while values <0.1 or >0.9 suggested poor model fit (Hobbs & Hooten, 2017). We used Watanabe–Akaike Information Criterion (WAIC) for model selection, where lower WAIC values indicate better predictive performance (Hooten & Hobbs, 2015). To further evaluate the predictive ability and complexity of the models, we also report elpd (Expected Log Pointwise Predictive Density), with higher values reflecting better predictive performance, and pD (effective number of parameters),

where low pD values indicate more parsimonious models. The ideal model therefore has a high elpd and a relatively low pD.

2.7 | *Trypanosoma* prevalence

To analyse the relationships between local and landscape attributes and site-level parasite infection, we ran generalized additive mixed models (GAMMs) for *T. cruzi* infection prevalence among the palms sampled, which also accounted for the spatial autocorrelation (Hastie & Tibshirani, 1990). Importantly, these models were exclusively based on palm trees that were occupied by *R. pallescens* during the study period, including both infected and uninfected individuals (diagnosis provided by RT-PCR). We modelled the smooth effects of continuous covariates in the «mgcv» package v. 1.8-28 in R statistical data analysis software (https://cran.r-project.org/web/packages/mgcv/index.html). Specifically, covariates included palm-level characteristics and forest cover within 300 m. The models were fitted using regression P-splines for smooth terms. We considered the following smoothing terms to select the best model fit: (i) thin plate regression splines; (ii) Duchon splines; (iii) cubic regression splines; (iv) B-splines; and (v) P-splines. The knot-based penalized cubic regression splines showed the best performance. Spatial coordinates were included to account for spatial autocorrelation, with a smoothing spline applied. Response variables corresponded to prevalence (presence or absence) of *T. cruzi*. For all GAMs, we used a binomial distribution, Palm ID as a random factor and included Triatomine developmental stage as a fixed factor. Model fit with observed data was assessed using Akaike information criterion (AIC) value and the percentage of total deviance explained. Model residuals were inspected using graphical methods by plotting randomized quantile residuals versus linear predictor. The effective degrees of freedom (edf) for smooth terms were used to assess their complexity, with values greater than 1 indicating nonlinear relationships between predictors and the response variable. We report explained deviance (45.4%) indicators of the explained variation of the full model. The model performance was checked using Q-Q plot of deviance residual of the best model (Figure S6).

We analysed spatial variation in parasitism using Moran's *I* to test for spatial autocorrelation and confirm independence between observations using the function moran.test () in the «spdep» package. We calculated and compared geographic distances and dissimilarity in the rate of parasitism for each parasite species at a given site using the five nearest neighbours. A statistically significant ($p < 0.05$) Moran's *I* above 0 (Moran's $I > 0$) indicated a spatial 'aggregation' pattern or risk zone.

3 | RESULTS

3.1 | Field and landscape observations

We detected *R. pallescens* in 24 of the 46 palms (52%) across the 11 communities; these 46 palms had a mean stem height of 3.8 m (SD 0.87 m; range 2.38–6.7 m), a mean infructescence score of one and a mean DOM score of one unit (SD 0.5; range 1–3). We collected a total of 160 triatomes over the study period; Figure S5 shows the *R. pallescens* geographic origin and developmental stages. The three locations with the highest number of bugs were dominated by secondary forest and together accounted for 60% of all collected samples.

3.2 | Site-occupancy analysis

The estimated average triatomine occupancy per palm of 0.62 was higher than the naïve (raw) occupancy rate (0.52). Regarding our site-occupancy models, we found that the daily maximum temperature during sampling was the most important detection covariate (WAIC = 191.82, Bayesian *p*-value = 0.44; Table 1) and was associated with significantly lower *R. pallescens* detectability (Estimate = −0.65, SD = 0.21; Figure 3a). Our models also demonstrated that maximum, minimum and average temperatures negatively correlated with detectability, whereas higher precipitation increased detectability (Estimate = 0.61, SD = 0.21). Notably, the models incorporating average temperature and precipitation also showed strong fits, as their ΔWAIC values were close to that of the best-fitting model. This underlines the importance of these climatic variables, measured at the used spatial and temporal scales, as informative predictors of *R. pallescens* detectability across the landscape. After accounting for detection probability, *R. pallescens* palm occupancy changed with

Covariate	Mean (SD)	Bayesian *p*-value	pD	elpd	WAIC	ΔWAIC
ρ~Max. Temp	−0.65 (0.21)	0.44	6.7	−89.2	**191.82**	
ρ~Ave. Temp	−0.69 (0.23)	0.55	7.35	−88.93	192.56	0.74
ρ~Precipitation	0.61 (0.21)	0.46	7.21	−89.61	193.66	1.84
ρ~Min. Temp	−0.15 (0.23)	0.49	7.35	−94.38	203.46	11.64

Note: In the table are shown the WAIC (Watanabe-Akaike Information Criterion), ΔWAIC (the difference between the WAIC value of a given model and the lowest WAIC value among all the models being compared), elpd (expected log pointwise predictive density), pD (effective number of parameters). Bayesian *p*-value is a model fit statistic calculated using the Freeman–Tukey discrepancy measure, where values near 0.5 indicate good fit and values below 0.1 or above 0.9 suggest poor model fit. Bold indicates lower value.

TABLE 1 Models of detection probability (p) for *Rhodnius pallescens*, with associated detection covariates: Accumulated daily precipitation (mm) during the sampling period ('precipitation'), maximum daily temperature (°C), minimum daily temperature (°C), and average daily temperature (°C).

Journal of Applied Ecology

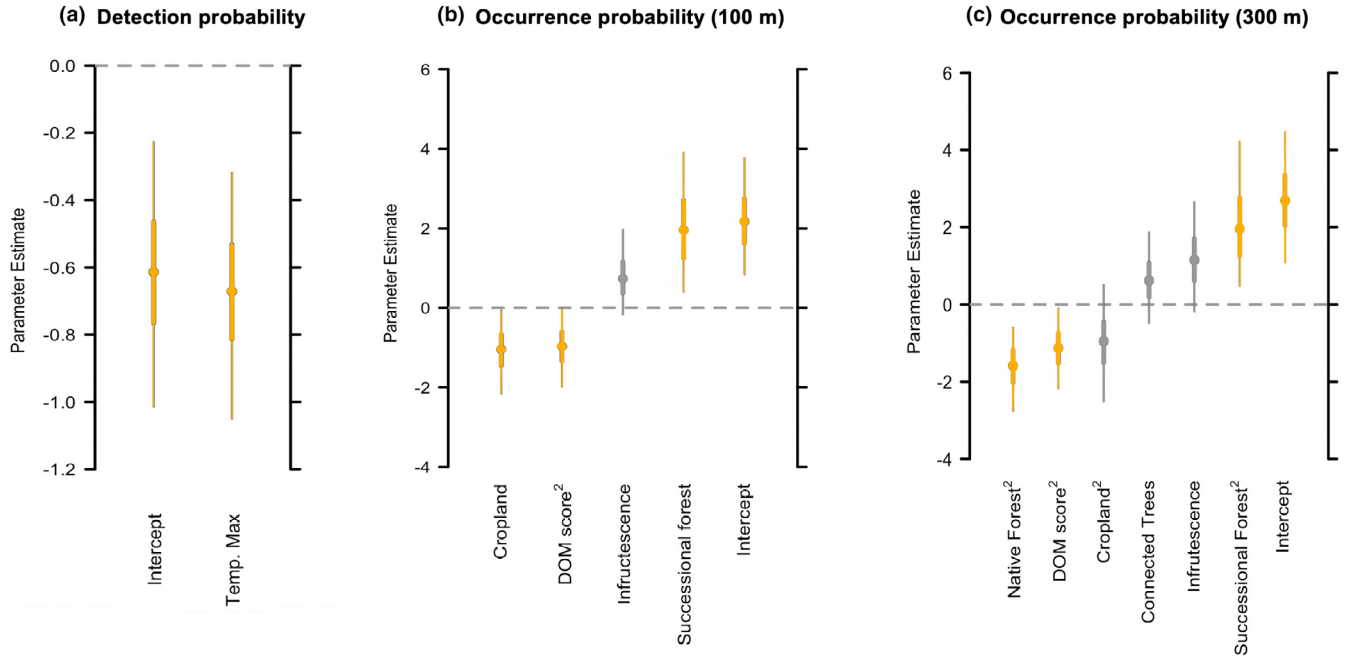


FIGURE 3 *Rhodnius pallescens* detection (a) and occurrence (b, c) parameter estimates, with upper and lower 90% credible intervals estimated from best site-occupancy models at different spatial extends at the study sites in Cocle, Panama. For occupancy probabilities, metrics were calculated at 100-m buffers (b) and 300-m buffers (c). Grey bars show relationships in which the 90% Bayesian credible interval (BCI) overlaps zero. Orange bars indicate that the 90% BCI does not overlap with zero (i.e. variable is a significant predictor of occupancy). Superscript 2 next to covariates indicates estimated quadratic effects. DOM scores refer to Dead Organic Matter scores for palm trees, according to Abad-Franch et al. (2005) as described in Section 2.

the LULC and palm-level traits (Tables S2 and S3). LULC metrics at all three spatial scales (100, 300 and 500 m) influenced *R. pallescens* occupancy (Tables S2 and S3). Models that accounted for spatial autocorrelation did not perform significantly better than nonspatial models (see Model Fit and Accuracy; Tables S2 and S3). We obtained a single final top-ranked dynamic occupancy model for each buffer size (Table S2) after our selection procedure and removal of models with uninformative covariables. Quadratic composition models performed better than linear composition terms among all spatial scales, indicating that the effect of most covariates is not linear.

Based on the β coefficient estimates of the additive version of our site-occupancy models (Table 2), the best models that explained *Rhodnius* occupancy included landscape variables estimated at a scale of 300 m (Tables S2 and S3) and identified the best predictors of *R. pallescens* occupancy to be a combination of land use cover and palm-level traits. According to the top-ranked model, vector occupancy was significantly higher (90% BCIs that did not include 0) with intermediate proportions of successional forest (Estimate = 2.08, SD = 1.07). We considered other covariates to be biologically meaningful because, although their 90% credible intervals included zero, their 75% credible intervals did not, including the amount of infructescence (Estimate = 1.17, SD = 0.8) and the number of connected trees (Estimate = 0.64, SD = 0.66) (Figure 3c). *Rhodnius pallescens* occurrence decreased with an increasing percentage of surrounding native forest land category (90% BCIs did not include 0) in a nonlinear manner (Estimate = −1.61, SD = 90), suggesting that *R. pallescens* are less likely to occupy areas highly dominated by native forest and arid areas. Also, we considered the negative effect of DOM score (Estimate = −1.13, SD = 0.90) and the percent Cropland (Estimate = −0.97, SD = 0.59) to be biologically meaningful of *R. pallescens* occupancy as their 75% BCIs did not overlap with 0 (Figure 3b). To supplement the credible intervals depicted in Figure 3, detailed credible interval values (4%, 25%, 50%, 75% and 90%) for all occurrence model parameters on the logit scale are provided in Table S3.

3.3 | Infection prevalence

RT-PCR assays detected *T. cruzi* infection in 70% of bugs overall. Infected individuals were found across all developmental stages. *Trypanosoma cruzi* and *T. rangeli* infection changed with triatomine developmental stage (Figure 4). Co-infections with *T. cruzi* and *T. rangeli* were proportionally higher in the adult stage than in the nymphal instars.

A complete list of the GAMMs models evaluated is shown in (Table 3). The best-fit model predicting *T. cruzi* infection in kissing bugs is described in the Supporting Information S3.

The best-fit GAM model shows a significant association between *T. cruzi* infection and the smoothed effects of native forest percent (edf: 2.30; *p*-value = 0.005) and per cent of grassland (edf: 3.94; *p*-value = 0.033) (Table 4). After plotting the partial effect of each variable included in our best GAM model, we observed a positive association between native forest and grassland coverage

TABLE 2 Comparison of additive occupancy (ψ) models for *Rhodnius pallescens* that include covariates using fine resolution (10 m) land cover spatial data.

Model	Bayesian *p*-value	WAIC	ΔWAIC	Covariates	Estimate	SD	Rhat
Best additive (300 m)	0.46	178.48		Successional (300 m)[a]	2.08	1.07	1
				Native (300 m)[a]	−1.61	0.61	1
				Cropland (300 m)[a]	−0.97	0.59	1
				DOM score[a]	−1.13	0.9	1
				Infructescence	1.17	0.8	1
				Connected trees	0.64	0.66	1
Best additive (100 m)	0.47	183	4.52	Successional (100 m)	1.81	1.02	1
				Cropland (100 m)	−1.08	0.6	1
				DOM score[a]	−0.97	0.55	1
				Infructescence	0.79	0.61	1
Null	0.44	191.82	17.34	~1			

Note: In the table are shown the WAIC (Watanabe-Akaike Information Criterion), ΔWAIC (the difference between the WAIC value of a given model and the lowest WAIC value among all the models being compared). Bayesian *p*-value is a model fit statistic calculated using the Freeman–Tukey discrepancy measure, where values near 0.5 indicate good fit and values below 0.1 or above 0.9 suggest poor model fit. The R-hat statistic assesses the convergence of Markov Chain Monte Carlo (MCMC) simulations; values close to 1 indicate that the simulations have converged.

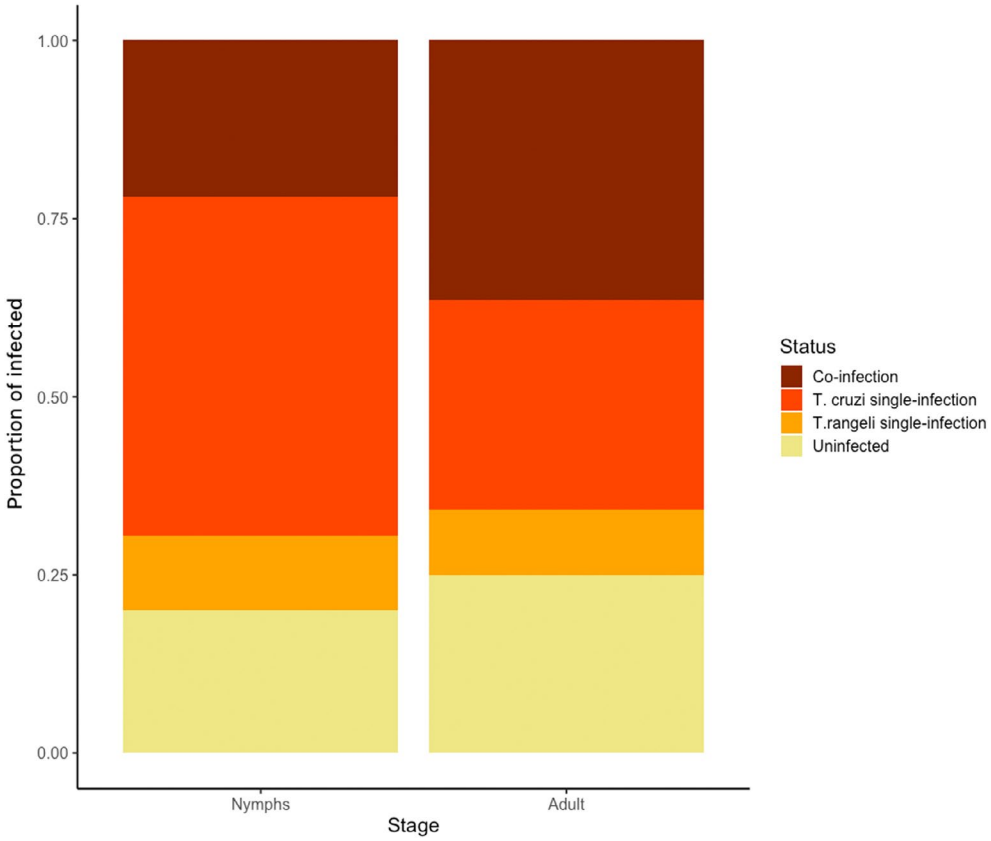


FIGURE 4 Infection prevalence: The stacked bar charts show proportion values for circulating *Trypanosoma cruzi* and *Trypanosoma rangeli* single infections and co-infections in *Rhodnius pallescens* split by developmental stages.

percentages with infection status (above zero) after crossing intermediate values. Both native forest and grassland cover with edf values above 2 were strongly nonlinearly associated with *T. cruzi* infection. The smoothed term of daily precipitation was weakly nonlinearly associated with *T. cruzi* infection (Table 4). In our best GAM model, spatial coordinates, modelled as a two-way tensor interaction, were significant predictors of *T. cruzi* infection in *R. pallescens* (edf: 2.30; $p = 0.046$; Figure 5). Panel c in Figure 5

Journal of Applied Ecology

TABLE 3 Comparison of generalized additive mixed-effects models (GAMM) using a model selection approach.

Model	Factors	Covariates	Adjusted R^2	Deviance explained	AIC	ΔAIC
Best additive	Palm ID+ Stage	~Nat + Gras + Prec + (*X*, *Y*) + ConTre	0.38	45.20%	143.48	
GAM additive 1	Palm ID+ Stage	~Arti + Succ + Gras + Prec + (*X*, *Y*) + infruc + DOM + ConTre	0.33	40%	147.89	4.41
Global	Palm ID+ Stage	~Arti + Succ + Nat + Gras + Prec + (*X*, *Y*) + infruc + DOM + ConTre + Elev	0.38	49.40%	149.85	6.37
Null	—	~1	−2.22E-16	−1.73E-15	182.83	39.35

Note: The best GAMM model was selected using a stepwise procedure and the lowest values of AIC and global deviance. Abbreviations of predictors: (*X*, *Y*), latitude and longitude; Arti, artificial surfaces; ConTre, number of connected trees; Gras, grassland; infruc, infructescence; Nat, native forest; Prec, daily precipitation; Succ, successional forest.

TABLE 4 Model parameter estimates for the best-fitted generalized additive model looking at the effect of landscape composition at 300-m buffers and palm traits on infection status with *Trypanosoma cruzi* (presence/absence) of *Rhodnius pallescens*.

	AIC = 143.48		
Total explained = 45.2%	**Estimate**	**edf**	***p*-value**
Fixed terms			
Number of connected trees	−1.04		*0.05*
Stage (Nymph 2)	1.7		*0.04*
Smooth terms			
Grassland		3.94	*0.03*
Native forest		2.3	*<0.01*
Daily precipitation		4.97	0.17
Long, Lat		4	*0.04*

Note: Estimate, estimated degrees of freedom, and *p*-values are shown for each predictor. The 'edf' (effective degrees of freedom) indicates the complexity of the smooth terms, where values greater than 1 suggest a nonlinear relationship between the predictor and the response. Italics denotes significant values.

illustrates that the spatial interaction between longitude and latitude drives localized variation in infection probability beyond the main effects, with warm and cool colours indicating areas of higher and lower predicted risk, respectively.

Our best-fit model had a cross-validated performance score (area under the receiver operator characteristic curve, ROC AUC) of 0.90 (Figures S6 and S7), indicating good model prediction probabilities. The estimated spline terms for native forest, grassland and spatial coordinates (Figure 5) showed distinct patterns, suggesting their effects changed across different variable ranges. The bottom panel of Figure 5 presents the two-dimensional smoothing of the tensor product for spatial coordinates, highlighting spatial variability in *T. cruzi* infection. This pattern aligns with the Moran's *I* test, which detected a positive but weak spatial autocorrelation for *T. cruzi* infection ($I = 0.11$, $p = 0.004$), but no significant autocorrelation for *T. rangeli* ($I = 0.009$, $p = 0.34$). Moreover, we found no strong associations between *T. rangeli* infection and the environmental, land cover, palm trait or climatic variables examined.

4 | DISCUSSION

Our results indicate that the landscape composition surrounding *Attalea* palms is a complex mosaic of human-influenced environmental variables that influences Chagas disease transmission in distinct ways. This study shows that fine-scale rural land cover variables play an important role in the spatial distribution of *R. pallescens*; particularly, a greater percent cover of successional forest increases the likelihood of vector occurrence, while the higher percentage of native forest decreases the likelihood of their presence; the spatial scale of the analysis affects our ability to identify and quantify the land cover-triatomine occurrence relationship; and (3) triatomine infection with *T. cruzi* is not spatially uniform, in particular, native forest and grassland cover increases the probability of *T. cruzi* infection in triatomines after intermediate levels of cover have been reached.

Our findings align with past work showing that anthropogenic landscape changes at fine-scales, climatic conditions and microhabitat characteristics influence triatomine population occurrence in Neotropical rural environments (Gottdenker et al., 2012; Urbano et al., 2015; Kilpatrick et al., 2017; Rodríguez et al., 2018; Santos et al., 2021; Varian et al., 2023). Sylvatic triatomines can fly into homes from nearby palm trees, which can lead to new cases of Chagas disease in humans. Determining which characteristics cause palms to be more frequently infested may contribute to disease prevention strategies (Abad-Franch et al., 2015). In terms of spatial scale, our occupancy models using land cover data within a 300-m buffer outperformed those using a 100-m buffer. This aligns with findings by Castro et al. (2014), who reported that the average flight distance of *R. pallescens*, was less than 300 m, suggesting this distance as a typical flight range. Ecological traits of *R. pallescens* may be shaped by environmental conditions at this spatial scale (Coutts et al., 2021). However, it is important to keep in mind that analyses of anthropogenic modifications at a single scale may obscure key patterns, as biotic factors vary more at smaller scales and climactic factors at larger ones (Cohen et al., 2016).

4.1 | Landscape composition and palm traits influence vector occurrence

Our models showed that *R. pallescens* occurrence peaked at intermediate amounts of forest cover and palm traits, rather than in a linear

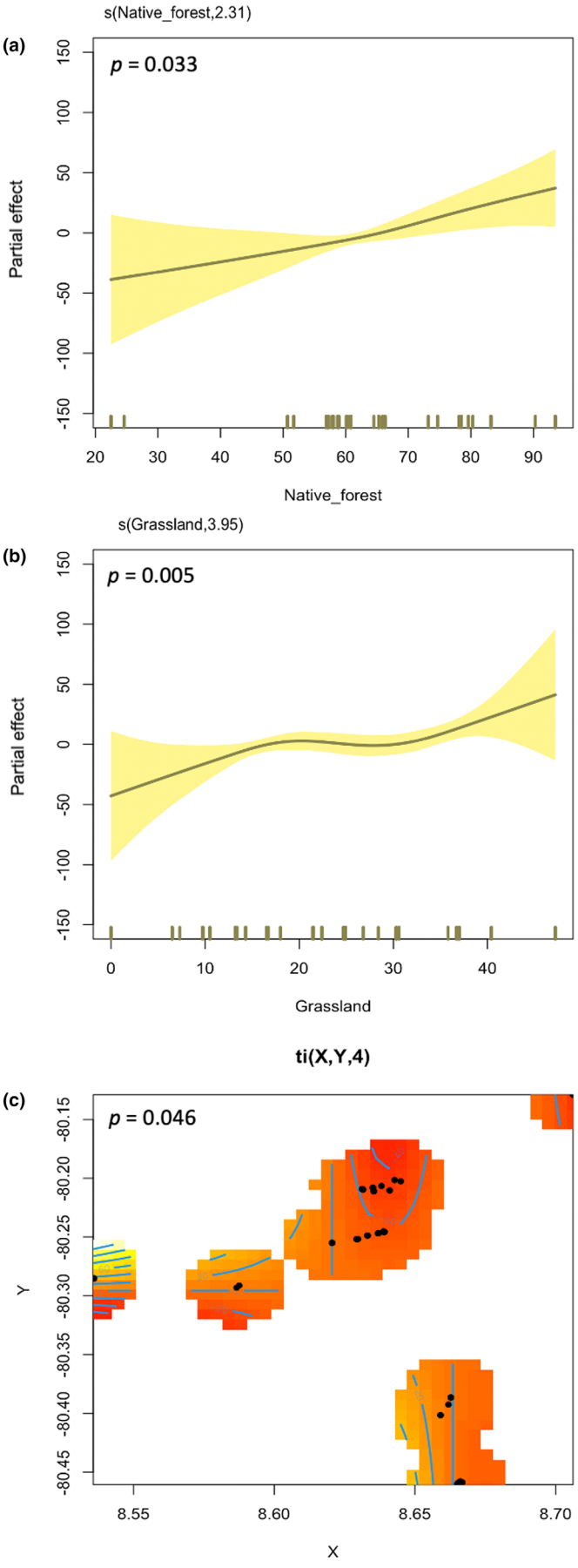

s(Native_forest,2.31)
(a)
p = 0.033
Partial effect
Native_forest
s(Grassland,3.95)
(b)
p = 0.005
Partial effect
Grassland
ti(X,Y,4)
(c)
p = 0.046
Y
X

FIGURE 5 Generalized additive mixed model plots showing the partial effects of selected explanatory variables on the infection status with *Trypanosoma cruzi*. Panel (a) shows the effect of percent of native forest, (b) percent of Grassland. In panels (a, b), the *y*-axis represents the partial effect of each variable. The tick marks on the *x*-axis are observed data points and (c) spatial coordinates. Dots are partial residuals, and the shaded areas indicate the 95% confidence intervals.

fashion, and that native forest and reforestation areas (as a percentage of successional forest) are important habitat features for predicting the species' presence. First, we observed that higher amounts of native forest surrounding a focal palm are associated with a lower kissing bug occurrence. Extensive areas of forest along with other aspects of landscape configuration are essential for maintaining specialist species (Gottdenker et al., 2011). A higher proportion of native forest cover could maintain a stable food web structure, where the potential presence of natural enemies, predators and pathogens of *R. pallescens* may lead to lower vector abundance (Varian et al., 2023; Teixeira et al., 2001). Second, there is a positive association with the proportion of regenerating or successional forest and the probability of palm infestation. This could be related to the increased number of forest edges in regenerating forests which can increase the abundance of reservoirs and vectors, creating corridors for their movement (Faust et al., 2018; Prist et al., 2022). Our findings show similar patterns to what has been found for *Rhodnius* spp. in Panama and Brazil, where triatomines were more frequent in palms located in landscapes altered by human activities, such as areas with remnants of secondary vegetation and young secondary forest (Gottdenker et al., 2011; Julião et al., 2021).

Palm structural complexity also influenced vector presence due to: (Abad-Franch et al., 2005) complex palm crowns attracting vertebrate hosts from which vectors can feed (Abad-Franch et al., 2010; Ricardo-Silva et al., 2012) intricate crowns create stable microclimates in palm crowns favouring insect survival (Urbano et al., 2015); and (Abad-Franch et al., 2015) palm structural features providing triatomine oviposition sites (Abad-Franch et al., 2010). Among the palm traits, infructescence and DOM score significantly affected bug presence. Infructescence positively influenced bug presence, consistent with Varian et al. (2023) and Rodríguez et al. (2018) who found higher *R. pallescens* infestation in palms with more fruit. Palm fruits are key food sources for many terrestrial mammals (Terborgh, 1986), and their abundance can attract arboreal vertebrates, thereby increasing food sources for triatomines, while seasonal variation in fruiting shapes local mammal communities (Silvius, 2002).

Conversely, DOM score negatively affected bug presence. Although Varian et al. (2023) noted that 'high-risk' palms had more DOM, its type and quality of organic material (e.g. leaf litter, fibres, animal remains) may influence shelter suitability differently by altering microhabitats. These effects likely vary with host dynamics, temporal habitat shifts and broader microclimatic factors such as precipitation, shading and temperature, which can shape triatomine presence.

4.2 | Parasite infection, spatial patterns and landscape determinants

Trypanosoma cruzi dominated *R. pallescens* infection (~70%) and approximately 40% of the bugs were infected with *T. rangeli*, similar to results from the western border of the Panama Canal (Calzada et al., 2006); but lower than the prevalence in the Eastern border of the Panama Canal, with 80% and 90% infection (Pineda et al., 2008; Vasquez et al., 2004). Similar to other *R. pallescens* populations (Gottdenker et al., 2016), our study showed more frequent co-infection in adults versus nymphs, possibly driven by *T. cruzi* and *T. rangeli* co-infecting increasing vector fitness, as shown in other *Rhodnius* species (Peterson et al., 2016). Co-infection by these two parasites can improve vector fitness by reducing the negative effects typically caused by single infections if mutual competitive suppression or immunologically modulated interactions occur between parasites (Balmer et al., 2009). This interaction may help offset the fitness costs associated with single infections, allowing more virulent strains to persist and potentially increasing the transmission potential of both parasites.

Trypanosoma cruzi infection rates are affected by variations in pathogen–reservoir host interactions as the environment changes (Gurgel-Gonçalves et al., 2003). Landscape variables, particularly in fragmented landscapes, can often show nonlinear relationships with infection metrics (Tracey et al., 2014; White et al., 2018). Our GAMM models indicated that the percentage of native forest has a partial positive effect on the probability of parasite infection after intermediate levels (>60%) and that grassland percentage also influences infection probability, with a positive but highly nonlinear effect. In different areas in Panama, Varian et al. (2023) found that the proportion of *R. pallescens* infected with *T. cruzi* was typically higher in forest remnants. Our findings suggest that multiple factors may interact with land cover to influence infection rates. For instance, the number of connected palm trees seems to increase with native forest cover, likely supporting a higher abundance of vertebrate hosts that use palms for nesting, roosting, or foraging—thereby raising infection probabilities. On the other hand, the number of connected palms in our study area seems to decrease with the percentage of grassland, making the remaining palms potential refuges for synanthropic mammals such as opossums that can have higher rates of *T. cruzi* infection in disturbed habitats, facilitating vector infection by the parasite.

4.3 | From palm data to an integrated land management for vector-borne disease mitigation

Our results underscore the complex relationship between vegetation cover, the presence of palm trees, climatic conditions and *T. cruzi* infection in triatomines. Here, the percentage of native forest was negatively associated with *Rhodnius* occurrence but positively associated with *T. cruzi* infection. This multidirectionality of effects has been evidenced in other similar systems; for example, Dumonteil and Gourbiére (2004) found a higher abundance of kissing bugs associated with disturbed vegetation. Conversely, greater kissing bug

occurrence in homes was associated with the presence of tall forests. Similarly, in other vector systems, such as mosquitoes, there is evidence that increased intensity of forest management reduces vector abundance yet increases Haemosporidian infections in the vectors (Van Hoesel et al., 2019). Opposing effects such as these could complicate efforts to predict and mitigate vector-borne diseases. While we acknowledge that our sampling size was relatively small, our field effort was comparable to or even exceeded that of previous studies conducted in nearby areas of the Canal region (Gottdenker et al., 2011). Thus, the number of samples primarily reflects the naturally lower abundance observed at our study. Based on these findings and considering the social and agricultural context of the region, we suggest that in rural tropical landscapes such as those in Panama, successional forests may represent higher-risk environments due to greater *R. pallescens* densities and frequent human activity linked to farming and resource use, which together increase opportunities for human–vector contact near communities and forest edges.

Taken together, these findings reinforce the idea that the transmission of Chagas disease arises from a complex network of ecological and socio-environmental interactions, instead of few directional relationships (Fernández et al., 2019; Brito et al., 2024). This complexity calls for integrative and multiscale strategies, in both research and management, that encompass vector biology, reservoir diversity, land use patterns and anthropogenic disturbances, to effectively mitigate *T. cruzi* transmission. While reforestation is important for ecosystem restoration and long-term environmental health, our findings indicate that reforestation can initially increase vector abundance, potentially raising short-term infection risks. Therefore, promoting the maturation of existing forests should be a priority to reach a more stable ecological state where vector abundance declines even as infection prevalence stabilizes. These insights can guide land use planning towards reforestation and vegetation management practices that help minimize *T. cruzi* transmission risks. Reforestation efforts might be more prudent if focused in areas farther from human settlements, minimizing immediate contact between infected vectors and people. Additionally, complementing landscape management with direct prevention strategies, such as installing window screens, use of mosquito nets, improving housing infrastructure and community education on reducing domestic triatomine exposure—can provide more immediate protection against human–vector contact. The predictive model developed in this study can also assist health authorities in identifying high-risk areas for targeted vector monitoring and surveillance. These results should serve as a basis for future studies and guide coherent prevention strategies adapted to the unique socio-ecological contexts.

AUTHOR CONTRIBUTIONS

Nicole L. Gottdenker, Sonia Altizer, Azael Saldaña, Jose E. Calzada and Juliana Hoyos conceived the idea with input from all authors. Azael Saldaña, Kadir Gonzalez, Vanessa Pineda, Juliana Hoyos and Daniel Mendieta collected data. Juliana Hoyos and Vanessa Pineda performed molecular biology experiments. Juliana Hoyos analysed the data. Juliana Hoyos and Alberto Cumbrera performed landscape analysis. Juliana Hoyos led the writing of the manuscript. Juliana Hoyos, Sonia Altizer, Nicole L. Gottdenker, Raissa Nogueira de Brito and Susan Tanner drafted the article and revised it critically for important intellectual content. All authors provided critical feedback and approved the final submitted version.

ACKNOWLEDGEMENTS

We acknowledge funding from the National Science Foundation NSF CNH2-1924200 and the University of Georgia. Any opinions, findings and conclusions or recommendations expressed in this material are those of the authors and do not necessarily reflect the views of the National Science Foundation. Juliana Hoyos was partially funded by Grant/Award Number 2018/20695-7; Ministerio de Ciencia, Tecnología e Innovacion de Colombia (MinCiencias), Grant/Award Numbers: Convocatoria Doctorados en el Exterior 906. Azael Saldaña, Kadir Gonzalez, and Jose E. Calzada are members and received financial support from the Sistema Nacional de Investigación (SNI), SENACYT, Panama.

CONFLICT OF INTEREST STATEMENT

The authors confirm that they have no conflict of interest to disclose.

DATA AVAILABILITY STATEMENT

Occurrence data and covariates used in this study are available through the Zenodo repository: https://doi.org/10.5281/zenodo.17793667 (Hoyos et al., 2025). Original R scripts used for data processing, modelling and figure generation are archived on Zenodo within the same record.

ORCID

Juliana Hoyos https://orcid.org/0000-0003-3270-0135

REFERENCES

Abad-Franch, F., Ferraz, G., Campos, C., Palomeque, F. S., Grijalva, M. J., Aguilar, H. M., & Miles, M. A. (2010). Modeling disease vector occurrence when detection is imperfect: Infestation of Amazonian palm trees by Triatomine bugs at three spatial scales. *PLoS Neglected Tropical Diseases*, *4*(3), e620. https://doi.org/10.1371/journal.pntd.0000620

Abad-Franch, F., Lima, M. M., Sarquis, O., Gurgel-Gonçalves, R., Sánchez-Martín, M., Calzada, J., Saldaña, A., Monteiro, F. A., Palomeque, F. S., Santos, W. S., Angulo, V. M., Esteban, L., Dias, F. B. S., Diotaiuti, L., Bar, M. E., & Gottdenker, N. L. (2015). On palms, bugs, and Chagas disease in the Americas. *Acta Tropica*, *151*, 126–141. https://doi.org/10.1016/j.actatropica.2015.07.005

Abad-Franch, F., Palomeque, F. S., Aguilar, H. M., & Miles, M. A. (2005). Field ecology of sylvatic *Rhodnius* populations (Heteroptera, Triatominae): Risk factors for palm tree infestation in Western Ecuador. *Tropical Medicine & International Health*, *10*(12), 1258–1266. https://doi.org/10.1111/j.1365-3156.2005.01511.x

Athni, T. S., Shocket, M. S., Couper, L. I., Nova, N., Caldwell, I. R., Caldwell, J. M., Childress, J. N., Childs, M. L., De Leo, G. A., Kirk, D. G., MacDonald, A. J., Olivarius, K., Pickel, D. G., Roberts, S. O., Winokur, O. C., Young, H. S., Cheng, J., Grant, E. A., Kurzner, P. M., … Mordecai, E. A. (2021). The influence of vector-borne disease on

human history: Socio-ecological mechanisms. *Ecology Letters*, *24*(4), 829–846. https://doi.org/10.1111/ele.13675

Balmer, O., Stearns, S. C., Schötzau, A., & Brun, R. (2009). Intraspecific competition between co-infecting parasite strains enhances host survival in African trypanosomes. *Ecology*, *90*(12), 3367–3378. https://doi.org/10.1890/08-2291.1

Botero, A., Ortiz, S., Muñoz, S., Triana, O., & Solari, A. (2010). Differentiation of *Trypanosoma cruzi* and *Trypanosoma rangeli* of Colombia using minicircle hybridization tests. *Diagnostic Microbiology and Infectious Disease*, *68*, 265–270. https://doi.org/10.1016/j.diagmicrobio.2010.06.020

Brito, R. N., Tanner, S., Runk, J. V., & Hoyos, J. (2024). Looking through the lens of social science approaches: A scoping review of leishmaniases and Chagas disease research. *Acta Tropica*, *249*, 107059. https://doi.org/10.1016/j.actatropica.2023.107059

Burkett-Cadena, N. D., & Vittor, A. Y. (2018). Deforestation and vector-borne disease: Forest conversion favors important mosquito vectors of human pathogens. *Basic and Applied Ecology*, *26*, 101–110. https://doi.org/10.1016/j.baae.2017.09.012

Calderón, J. M., & González, C. (2020). Co-occurrence or dependence? Using spatial analyses to explore the interaction between palms and *Rhodnius triatomines*. *Parasites & Vectors*, *13*(1), 211. https://doi.org/10.1186/s13071-020-04088-0

Calzada, J. E., Pineda, V., Montalvo, E., Alvarez, D., Santamaría, A. M., Samudio, F., Bayard, V., Cáceres, L., & Saldaña, A. (2006). Human trypanosome infection and the presence of intradomicile *Rhodnius pallescens* in the western border of the Panama Canal, Panama. *The American Journal of Tropical Medicine and Hygiene*, *74*(5), 762–765.

Carcavallo, R. U., Franca, M., Salvatella, R., de Curto Casas, S., Sherlock, I., & Galvao, C. (1998). Habitats and related fauna. In *Atlas of Chagas disease vectors in the Americas. Volume II* (pp. 561–600). Editora Fiocruz.

Castro, L. A., Peterson, J. K., Saldana, A., Perea, M. Y., Calzada, J. E., Pineda, V., Dobson, A. P., & Gottdenker, N. L. (2014). Flight behavior and performance of *Rhodnius pallescens* (Hemiptera: Reduviidae) on a tethered flight mill. *Journal of Medical Entomology*, *51*(5), 1010–1018. https://doi.org/10.1603/me14014

Chazdon, R. L., Broadbent, E. N., Rozendaal, D. M. A., Bongers, F., Zambrano, A. M. A., Aide, T. M., Balvanera, P., Becknell, J. M., Boukili, V., Brancalion, P. H. S., Craven, D., Almeida-Cortez, J. S., Cabral, G. A. L., De Jong, B., Denslow, J. S., Dent, D. H., DeWalt, S. J., Dupuy, J. M., Durán, S. M., … Poorter, L. (2016). Carbon sequestration potential of second-growth forest regeneration in the Latin American tropics. *Science Advances*, *2*(5), e1501639. https://doi.org/10.1126/sciadv.1501639

Cohen, J. M., Civitello, D. J., Brace, A. J., Feichtinger, E. M., Ortega, C. N., Richardson, J. C., Sauer, E. L., Liu, X., & Rohr, J. R. (2016). Spatial scale modulates the strength of ecological processes driving disease distributions. *Proceedings of the National Academy of Sciences of the United States of America*, *113*(24), E3359–E3364. https://doi.org/10.1073/pnas.1521657113

Coutts, S. R., Quintana-Ascencio, P. F., Menges, E. S., Salguero-Gómez, R., & Childs, D. Z. (2021). Fine-scale spatial variation in fitness is comparable to disturbance-induced fluctuations in a fire-adapted species. *Ecology*, *102*(4), e03287. https://doi.org/10.1002/ecy.3287

Cucunubá, Z. M., Gutiérrez-Romero, S. A., Ramírez, J. D., Velásquez-Ortiz, N., Ceccarelli, S., Parra-Henao, G., Henao-Martínez, A. F., Rabinovich, J., Basáñez, M. G., Nouvellet, P., & Abad-Franch, F. (2024). The epidemiology of Chagas disease in the Americas. *The Lancet Regional Health - Americas*, *37*, 100881. https://doi.org/10.1016/j.lana.2024.100881

Dias, F. B., Paula, A. S., Belisário, C. J., Lorenzo, M. G., Bezerra, C. M., Harry, M., & Diotaiuti, L. (2011). Influence of the palm tree species on the variability of *Rhodnius nasutus* Stål, 1859 (Hemiptera, Reduviidae, Triatominae). *Infection, Genetics and Evolution*, *11*(5), 869–877. https://doi.org/10.1016/j.meegid.2011.02.008

Doser, J. W., Finley, A. O., Kéry, M., & Zipkin, E. F. (2022). spOccupancy: An R package for single-species, multi-species, and integrated spatial occupancy models. *Methods in Ecology and Evolution*, *13*, 1670–1678. https://doi.org/10.1111/2041-210X.13897

Dumonteil, E., & Gourbiére, S. (2004). Predicting *Triatoma dimidiata* abundance and infection rate: A risk map for natural transmission of Chagas disease in the Yucatan peninsula of Mexico. *The American Journal of Tropical Medicine and Hygiene*, *70*(5), 514–519.

Eisen, R. J., Kugeler, K. J., Eisen, L., Beard, C. B., & Paddock, C. D. (2017). Tick-borne zoonoses in the United States: Persistent and emerging threats to human health. *ILAR Journal*, *58*(3), 319–335. https://doi.org/10.1093/ilar/ilx005

Faust, C. L., McCallum, H. I., Bloomfield, L. S. P., Gottdenker, N. L., Gillespie, T. R., Torney, C. J., Dobson, A. P., & Plowright, R. K. (2018). Pathogen spillover during land conversion. *Ecology Letters*, *21*(4), 471–483. https://doi.org/10.1111/ele.12904

Fernández, M. D. P., Gaspe, M. S., Sartor, P., & Gürtler, R. E. (2019). Human *Trypanosoma cruzi* infection is driven by eco-social interactions in rural communities of the Argentine Chaco. *PLoS Neglected Tropical Diseases*, *13*(12), e0007430. https://doi.org/10.1371/journal.pntd.0007430

Ferraguti, M., Magallanes, S., Suarez-Rubio, M., Bates, P. J. J., Marzal, A., & Renner, S. C. (2023). Does land-use and land cover affect vector-borne diseases? A systematic review and meta-analysis. *Landscape Ecology*, *38*(10), 2433–2451. https://doi.org/10.1007/s10980-023-01746-3

Global Forest Watch. (2024). *Forest data for Panama — country dashboard* [Data set]. World Resources Institute. Retrieved August 12, 2024, from https://www.globalforestwatch.org/dashboards/country/PAN/3/?map

Global Modeling and Assimilation Office (GMAO). (2015). *MERRA-2 tavg1_2d_slv_Nx: 2d,1-hourly, time-averaged, single-level, assimilation, single-level diagnostics V5.12.4*. Goddard Earth Sciences Data and Information Services Center (GES DISC). Retrieved March 28, 2019, from https://doi.org/10.5067/VJAFPLI1CSIV

Gottdenker, N. L., Calzada, J. E., Saldaña, A., & Carroll, C. R. (2011). Association of anthropogenic land use change and increased abundance of the Chagas disease vector *Rhodnius pallescens* in a rural landscape of Panama. *The American Society of Tropical Medicine and Hygiene*, *84*(1), 70–77. https://doi.org/10.4269/ajtmh.2011.10-0041

Gottdenker, N. L., Chaves, L. F., Calzada, J. E., Peterson, J. K., Santamaría, A., Pineda, V., & Saldaña, A. (2016). *Trypanosoma cruzi* and *Trypanosoma rangeli* co-infection patterns in insect vectors vary across habitat types in a fragmented forest landscape. *Parasitology Open*, *2*, e10. https://doi.org/10.1017/pao.2016.9

Gottdenker, N. L., Chaves, L. F., Calzada, J. E., Saldaña, A., & Carroll, C. R. (2012). Host life history strategy, species diversity, and habitat influence *Trypanosoma cruzi* vector infection in changing landscapes. *PLoS Neglected Tropical Diseases*, *6*(11), e1884. https://doi.org/10.1371/journal.pntd.0001884

Gottdenker, N. L., Streicker, D. G., Faust, C. L., & Carroll, C. R. (2014). Anthropogenic land use change and infectious diseases: A review of the evidence. *EcoHealth*, *11*(4), 619–632. https://doi.org/10.1007/s10393-014-0941-z

Guhl, F., & Vallejo, G. A. (2003). *Trypanosoma* (*Herpetosoma*) *rangeli* Tejera, 1920: an updated review. *Memórias do Instituto Oswaldo Cruz*, *98*(4), 435–442. https://doi.org/10.1590/s0074-02762003000400001

Gurgel-Gonçalves, R., Palma, A. R., Menezes, M. N., Leite, R. N., & Cuba, C. A. (2003). Sampling *Rhodnius neglectus* in *Mauritia flexuosa* palm trees: A field study in the Brazilian savanna. *Medical and Veterinary Entomology*, *17*(3), 347–350. https://doi.org/10.1046/j.1365-2915.2003.00448.x

Hastie, T. J., & Tibshirani, R. J. (1990). *Generalized additive models*. Chapman and Hall.

Hobbs, N. T., & Hooten, M. (2017). *Bayesian models: A statistical primer for ecologists*. Princeton University Press. https://doi.org/10.23943/princeton/9780691159287.001.0001

Hooten, M. B., & Hobbs, N. T. (2015). A guide to Bayesian model selection for ecologists. *Ecological Monographs*, *85*, 3–28. https://doi.org/10.1890/14-0661.1

Hoyos, J., Saldaña, A., Altizer, S., Pineda, V., Gonzalez, K., Calzada, J. E., de Brito, R. N., Tanner, S., Mendieta, D., Cumbrera, A., & Gottdenker, N. (2025). Hierarchical models from "successional and native forest predict the occurrence and infection status of Chagas disease vectors in Panama" [Datasets]. *Zenodo*. https://doi.org/10.5281/zenodo.17793667

Julião, G. R., Pimentel, I. F., de França, A. K., Gil, L. H. S., Simplício, M. F., da Santos Silva, G. D., Katsuragawa, T. H., & de Souza Rodrigues, M. M. (2021). *Rhodnius* spp. infestation in palm trees and natural infection by *Trypanosoma cruzi* and *Trypanosoma rangeli* in periurban and rural areas of state of the Rondônia, in the Brazilian Amazon. *Acta Tropica*, *220*, 105963. https://doi.org/10.1016/j.actatropica.2021.105963

Keesing, F., Belden, L. K., Daszak, P., Dobson, A., Harvell, C. D., Holt, R. D., Hudson, P., Jolles, A., Jones, K. E., Mitchell, C. E., Myers, S. S., Bogich, T., & Ostfeld, R. S. (2010). Impacts of biodiversity on the emergence and transmission of infectious diseases. *Nature*, *468*(7324), 647–652. https://doi.org/10.1038/nature09575

Keesing, F., & Ostfeld, R. S. (2021). Impacts of biodiversity and biodiversity loss on zoonotic diseases. *Proceedings of the National Academy of Sciences of the United States of America*, *118*(17), e2023540118. https://doi.org/10.1073/pnas.2023540118

Kilpatrick, A. M., Dobson, A. D. M., Levi, T., Salkeld, D. J., Swei, A., Ginsberg, H. S., Kjemtrup, A., Padgett, K. A., Jensen, P. M., Fish, D., Ogden, N. H., & Diuk-Wasser, M. A. (2017). Lyme disease ecology in a changing world: Consensus, uncertainty and critical gaps for improving control. *Philosophical Transactions of the Royal Society, B: Biological Sciences*, *372*(1722), 20160117. https://doi.org/10.1098/rstb.2016.0117

Lent, H., & Wygodzinsky, P. (1979). Revision of the Triatominae (Hemiptera, Reduviidae), and their significance as vectors of Chagas' disease. *Bulletin of the American Museum of Natural History*, *163*, 123–520.

MacDonald, A. J., & Mordecai, E. A. (2019). Amazon deforestation drives malaria transmission, and malaria burden reduces forest clearing. *Proceedings of the National Academy of Sciences of the United States of America*, *116*(44), 22212–22218. https://doi.org/10.1073/pnas.1905315116

MacKenzie, D. I., Nichols, J. D., Lachman, G. B., Droege, S., Royle, J. A., & Langtimm, C. A. (2002). Estimating site occupancy rates when detection probabilities are less than one. *Ecology*, *83*, 2248–2255.

MacKenzie, D. I., Nichols, J. D., Royle, J. A., Pollock, K. H., Bailey, L. L., & Hines, J. E. (2006). *Occupancy estimation and modeling: Inferring patterns and dynamics of species occurrence*. Academic Press.

Mertzlufft, C. E., Madden, M., Gottdenker, N. L., Velásquez Runk, J., Saldaña, A., Tanner, S., Calzada, J. E., & Yao, X. (2020). Landscape disturbance impacts on *Attalea butyracea* palm distribution in central Panama. *International Journal of Health Geographics*, *19*(1), 58. https://doi.org/10.1186/s12942-020-00244-y

Morand, S., & Lajaunie, C. (2021). Outbreaks of vector-borne and zoonotic diseases are associated with changes in forest cover and oil palm expansion at global scale. *Frontiers in Veterinary Science*, *8*, 661063. https://doi.org/10.3389/fvets.2021.661063

Muñoz-Calderón, A., Wehrendt, D., Cura, C., Gómez-Bravo, A., Abril, M., Giammaria, M., Lucero, R. H., & Schijman, A. G. (2020). Real-time polymerase chain reaction-based algorithm for differential diagnosis of kinetoplastidean species of zoonotic relevance. *Infection, Genetics and Evolution*, *83*, 104328. https://doi.org/10.1016/j.meegid.2020.104328

Noireau, F., Abad-Franch, F., Valente, S. A., Dias-Lima, A., Lopes, C. M., Cunha, V., Valente, V. C., Palomeque, F. S., de Carvalho-Pinto, C. J., Sherlock, I., Aguilar, M., Steindel, M., Grisard, E. C., & Jurberg, J. (2002). Trapping Triatominae in silvatic habitats. *Memórias do Instituto Oswaldo Cruz*, *97*(1), 61–63. https://doi.org/10.1590/s0074-02762002000100009

Pan American Health Organization. (2025). Chagas disease. https://www.paho.org/en/topics/chagas-disease#:~:text=Chagas%20disease%20is%20the%20most,the%20Rhodnius%20pallescens%20in%20Panama

Peterson, J. K., Graham, A. L., Elliott, R. J., Dobson, A. P., & Triana Chávez, O. (2016). *Trypanosoma cruzi-Trypanosoma rangeli* co-infection ameliorates negative effects of single trypanosome infections in experimentally infected *Rhodnius prolixus*. *Parasitology*, *143*(9), 1157–1167. https://doi.org/10.1017/S0031182016000615

Pineda, V., Montalvo, E., Alvarez, D., Santamaría, A. M., Calzada, J. E., & Saldaña, A. (2008). Feeding sources and trypanosome infection index of *Rhodnius pallescens* in a Chagas disease endemic area of Amador County, Panama. *Revista do Instituto de Medicina Tropical de São Paulo*, *50*(2), 113–116. https://doi.org/10.1590/s0036-46652008000200009

Poorter, L., van der Sande, M. T., Amissah, L., Bongers, F., Hordijk, I., Kok, J., Laurance, S. G., Martínez-Ramos, M., Matsuo, T., Meave, J. A., Muñoz, R., Peña-Claros, M., van Breugel, M., Herault, B., Jakovac, C. C., Lebrija-Trejos, E., Norden, N., & Lohbeck, M. (2024). A comprehensive framework for vegetation succession. *Ecosphere*, *15*(4), e4794. https://doi.org/10.1002/ecs2.4794

Prist, P. R., Siliansky de Andreazzi, C., Vidal, M. M., Zambrana-Torrelio, C., Daszak, P., Carvalho, R. L., & Tambosi, L. R. (2023). Promoting landscapes with a low zoonotic disease risk through forest restoration: The need for comprehensive guidelines. *Journal of Applied Ecology*, *60*(8), 1510–1521. https://doi.org/10.1111/1365-2664.14442

Prist, P. R., Tambosi, L. R., Mucci, L. F., Pinter, A., de Souza, R. P., Muylaert, R. L., Rhodes, J. R., Coutinho, C. H., Costa, L. F., D'Agostoni, T. L., Deus, J. T., Pavão, M., Port-Carvalho, M., Saad, L. D., Sallum, M. A. M., Spinola, R. M. F., & Metzger, J. P. (2022). Roads and forest edges facilitate yellow fever virus dispersion. *Journal of Applied Ecology*, *59*, 4–17. https://doi.org/10.1111/1365-2664.14031

Ricardo-Silva, A. H., Lopes, C. M., Ramos, L. B., Marques, W. A., Mello, C. B., Duarte, R., de la Fuente, A. L., Toma, H. K., Reboredo-Oliveira, L., Kikuchi, S. A., Baptista, T. F., Santos-Mallet, J. R., Junqueira, A. C., & Gonçalves, T. C. (2012). Correlation between populations of *Rhodnius* and presence of palm trees as risk factors for the emergence of Chagas disease in Amazon region, Brazil. *Acta Tropica*, *123*(3), 217–223. https://doi.org/10.1016/j.actatropica.2012.05.008

Roche, B., Rohani, P., Dobson, A. P., & Guégan, J. F. (2013). The impact of community organization on vector-borne pathogens. *The American Naturalist*, *181*(1), 1–11. https://doi.org/10.1086/668591

Rodríguez, I. G., Saldaña, A., González, K., Pineda, V., Perea, M., Santamaría, A. M., de Junca, C. C., Chaves, L. F., & Calzada, J. E. (2018). *Trypanosoma cruzi* infection in *Rhodnius pallescens* (Heteroptera: Reduviidae) infesting Coyol palms in the dry arch of Panamá. *Journal of Medical Entomology*, *55*(3), 691–700. https://doi.org/10.1093/jme/tjx249

Rozendaal, D. M. A., Bongers, F., Aide, T. M., Alvarez-Dávila, E., Ascarrunz, N., Balvanera, P., Becknell, J. M., Bentos, T. V., Brancalion, P. H. S., Cabral, G. A. L., Calvo-Rodriguez, S., Chave, J., César, R. G., Chazdon, R. L., Condit, R., Dallinga, J. S., de Almeida-Cortez, J. S., de Jong, B., de Oliveira, A., … Poorter, L. (2019). Biodiversity recovery of neotropical secondary forests. *Science Advances*, *5*(3), eaau3114. https://doi.org/10.1126/sciadv.aau3114

Santos, W. S., Gurgel-Gonçalves, R., Garcez, L. M., & Abad-Franch, F. (2021). Deforestation effects on *Attalea* palms and their resident *Rhodnius*, vectors of Chagas disease, in eastern Amazonia. *PLoS One*, *16*(5), e0252071. https://doi.org/10.1371/journal.pone.0252071

Silvius, K. M. (2002). Spatio-temporal patterns of palm endocarp use by three Amazonian forest mammals: Granivory or 'grubivory'? *Journal of Tropical Ecology*, *18*(5), 707–723. https://doi.org/10.1017/S0266467402002468

Skaff, N. K., Armstrong, P. M., Andreadis, T. G., & Cheruvelil, K. S. (2017). Wetland characteristics linked to broad-scale patterns in *Culiseta melanura* abundance and eastern equine encephalitis virus infection. *Parasites & Vectors*, *10*(1), 501. https://doi.org/10.1186/s13071-017-2482-0

Teixeira, A. R., Monteiro, P. S., Rebelo, J. M., Argañaraz, E. R., Vieira, D., Lauria-Pires, L., Nascimento, R., Vexenat, C. A., Silva, A. R., Ault, S. K., & Costa, J. M. (2001). Emerging Chagas disease: Trophic network and cycle of transmission of *Trypanosoma cruzi* from palm trees in the Amazon. *Emerging Infectious Diseases*, *7*(1), 100–112. https://doi.org/10.3201/eid0701.700100

Terborgh, J. (1986). Keystone plant resources in the tropical forest. In M. E. Soulé (Ed.), *Conservation biology: The science of scarcity and diversity* (pp. 330–344). Sinauer Associates.

Tonelli, A., Caceres-Escobar, H., Blagrove, M. S. C., Wardeh, M., & Di Marco, M. (2024). Identifying life-history patterns along the fast-slow continuum of mammalian viral carriers. *Royal Society Open Science*, *11*(7), 231512. https://doi.org/10.1098/rsos.231512

Tracey, J. A., Bevins, S. N., VandeWoude, S., & Crooks, K. R. (2014). An agent-based movement model to assess the impact of landscape fragmentation on disease transmission. *Ecosphere*, *5*, 1–24. https://doi.org/10.1890/ES13-00376.1

Urbano, P., Poveda, C., & Molina, J. (2015). Effect of the physiognomy of *Attalea butyracea* (Arecoideae) on population density and age distribution of *Rhodnius prolixus* (Triatominae). *Parasites & Vectors*, *8*, 199. https://doi.org/10.1186/s13071-015-0813-6

Van Hoesel, W., Marzal, A., Magallanes, S., Santiago-Alarcon, D., Ibáñez-Bernal, S., & Renner, S. C. (2019). Management of ecosystems alters vector dynamics and Haemosporidian infections. *Scientific Reports*, *9*(1), 8779. https://doi.org/10.1038/s41598-019-45068-4

Varian, C. P., Saldaña, A., Calzada, J. E., Abad-Franch, F., Kieran, T. J., Padukone, A., Peterson, J. K., & Gottdenker, N. L. (2023). Food web structure and microenvironment affect Chagas disease vector infection and abundance in a rural landscape. *Ecosphere*, *14*(1), e4347. https://doi.org/10.1002/ecs2.4347

Vasquez, A. M., Samudio, F. E., Saldaña, A., Paz, H. M., & Calzada, J. E. (2004). Eco-epidemiological aspects of *Trypanosoma cruzi*, *Trypanosoma rangeli* and their vector (*Rhodnius pallescens*) in Panama. *Revista do Instituto de Medicina Tropical de São Paulo*, *46*(4), 217–222. https://doi.org/10.1590/s0036-46652004000400008

Vaz, V. C., D'Andrea, P. S., & Jansen, A. M. (2007). Effects of habitat fragmentation on wild mammal infection by *Trypanosoma cruzi*. *Parasitology*, *134*(12), 1785–1793. https://doi.org/10.1017/S0031182007003230X

Vinatier, F., Gosme, M., & Valantin-Morison, M. (2013). Explaining host–parasitoid interactions at the landscape scale: A new approach for calibration and sensitivity analysis of complex spatio-temporal models. *Landscape Ecology*, *28*(2), 217–231. https://doi.org/10.1007/s10980-012-9822-4

Vinson, J. E., Gottdenker, N. L., Chaves, L. F., Kaul, R. B., Kramer, A. M., Drake, J. M., & Hall, R. J. (2022). Land reversion and zoonotic spillover risk. *Royal Society Open Science*, *9*(6), 220582. https://doi.org/10.1098/rsos.220582

White, L. A., Forester, J. D., & Craft, M. E. (2018). Disease outbreak thresholds emerge from interactions between movement behavior, landscape structure, and epidemiology. *Proceedings of the National Academy of Sciences of the United States of America*, *115*(28), 7374–7379. https://doi.org/10.1073/pnas.1801383115

Wright, S. J., Zeballos, H., Domínguez, I., Gallardo, M. M., Moreno, M. C., & Ibáñez, R. (2000). Poachers alter mammal abundance, seed dispersal, and seed predation in a neotropical forest. *Conservation Biology*, *14*(1), 227–239. https://doi.org/10.1046/j.1523-1739.2000.98333.x

SUPPORTING INFORMATION

Additional supporting information can be found online in the Supporting Information section at the end of this article.

Figure S1. Correlation analysis among the LULC types at 100 m.

Figure S2. Correlation analysis among the LULC types at 300 m.

Figure S3. Correlation analysis among the LULC types at 500 m.

Figure S4. Correlation analysis between independent covariates observed in the field sites and LULC types.

Figure S5. Abundance of Triatominae collected and subsequently analysed for *Trypanosoma* infection in each sampling; nymphal instars are indicated by N1–N5.

Table S1. Site-level covariates included in models to explain variation in occupancy and detectability of *R. pallescens*.

Table S2. Comparison of additive occupancy (ψ) models for *Rhodnius pallescens* using fine resolution (10 m^2) land cover spatial data.

Table S3. Quantiles of posterior distributions for occurrence model parameters on the logit scale associated with the additive occupancy (ψ) models for *Rhodnius pallescens* that include covariates from fine-resolution (10 m) land cover spatial data.

Figure S6. Quantile-quantile (Q-Q) graphical validation for the best-fitted GAMM model.

Figure S7. ROC curve for the best-fitted GAMM model.

How to cite this article: Hoyos, J., Saldaña, A., Altizer, S., Pineda, V., Gonzalez, K., Calzada, J. E., de Brito, R. N., Tanner, S., Mendieta, D., Cumbrera, A., & Gottdenker, N. L. (2026). Successional and native forests predict the occurrence and infection status of Chagas disease vectors in Panama. *Journal of Applied Ecology*, *63*, e70251. https://doi.org/10.1111/1365-2664.70251